#3616

Numerical Solutions of Navier-Stokes Equations for Push-Pull Flow

Z. Damin **K. Tsuji** **I. Fukuhara**

ABSTRACT

In this paper, the push-pull flow is assumed to be incompressible, two-dimensional, isothermal, laminar, and/or turbulent. By introducing the stream function and the vorticity, and by transforming Navier-Stokes equations into the equations of stream function and vorticity transportation, the problem of laminar flow is solved.

Since the Navier-Stokes equation is solved with time-mean computation, we try to solve the problem of turbulent flow with a one-equation model. The comparison between the computational results and the experimental data confirms the accuracy of the computation and the feasibility of the numerical analysis of the computer.

INTRODUCTION

Air curtains formed by the combination of push and pull flows are often used in air conditioning to insulate part of a space, such as gate air curtains for the prevention of the invasion of cold or warm air, and are used in factories to improve working environments by eliminating gas or fumes generated in many processes.

Owing to the complexity of the push-pull flow, research on the flow may be far from perfect until now. The formulae of its computation are essentially founded on the jet theories and/or experimental bases (Hayashi et al. 1985). In order to deepen our knowledge, the authors have been engaged in the computational analysis of push-pull flow.

Formerly, the computational analysis of incompressible flow was for solid boundaries. The boundary conditions could be assumed according to the Dirichlet conditions or the Neumann conditions.

Push-pull flows apart from the vicinity of the flanged opening are always in contact with flows such as polluting gases or transverse wind. The controlling ability of the push-pull flow determines whether the push flow entrained surrounding air or pollutant gases leaks from the inlet opening or not. This is reflected by the conditions of the free access of the flows at the nonsolid computational boundaries. The boundary with the distribution of velocity gradient which permits the free access of the flows is defined as free boundary by the authors.

Economization and efficiency must be pursued for any kind of push-pull flow installation. The main factor deciding the cost and effect is the ratio of flow rate. In other words, the ratio of the quantity of inlet, Q_3, to that of outlet, Q_1, reflects the controlling effect, the cost of operation, and initial investment. Now, the problem is how to determine the ratio of Q_3/Q_1.

In this paper, the method for determining the minimum flow ratio of both cases with or without flows disturbing push-pull flow is recommended. Using this method, the minimum flow ratio of more complicated cases can also be deduced. This will be discussed along with the experimental results.

The presence of the flange at the outlet adversely affects the fluidity of the outlet flow. The effects of the flange on the fluidity of the outlet flow are also discussed in the paper. The optimum combination of the outlet and the flange has been obtained by numerical analysis.

FLOW EQUATIONS

The steady two-dimensional flow of incompressible fluid can be expressed by the continuity equations and the Navier-Stokes equations. The dependent variable in these equations can be chosen as the stream function, ψ, and the vorticity, ω. Referring to the coordinates shown in Figure 1, if the width of outlet, D_1, is the reference width and the flow velocity at outlet, V_1, is the reference velocity, then, after dimensionless transformation, the fundamental $\psi-\omega$ equations describing laminar flows can be written as follows:

$$\frac{\partial^2\psi}{\partial x^2}+\frac{\partial^2\psi}{\partial y^2}=-\omega \tag{1}$$

$$\frac{\partial}{\partial x}\left(\omega\frac{\partial\psi}{\partial y}\right)-\frac{\partial}{\partial y}\left(\omega\frac{\partial\psi}{\partial x}\right)=\frac{1}{Re}\left(\frac{\partial^2\omega}{\partial x^2}+\frac{\partial^2\omega}{\partial y^2}\right) \tag{2}$$

where

$$u=\frac{\partial\psi}{\partial y},\quad v=\frac{\partial\psi}{\partial x},\quad \omega=\frac{\partial u}{\partial y}-\frac{\partial v}{\partial x} \tag{3}$$

For solving turbulent flow problems, the authors have tried both the one-equation model (k-L model) and the two-equation model (k-ϵ model) (Damin and Xinghua 1986). A

Z. Damin is Instructor, Hunan University, Changsha, Hunan, China; **K. Tsuji** is Associate Professor and **I. Fukuhara** is Assistant Professor, University of Osaka Prefecture, Osaka, Japan.

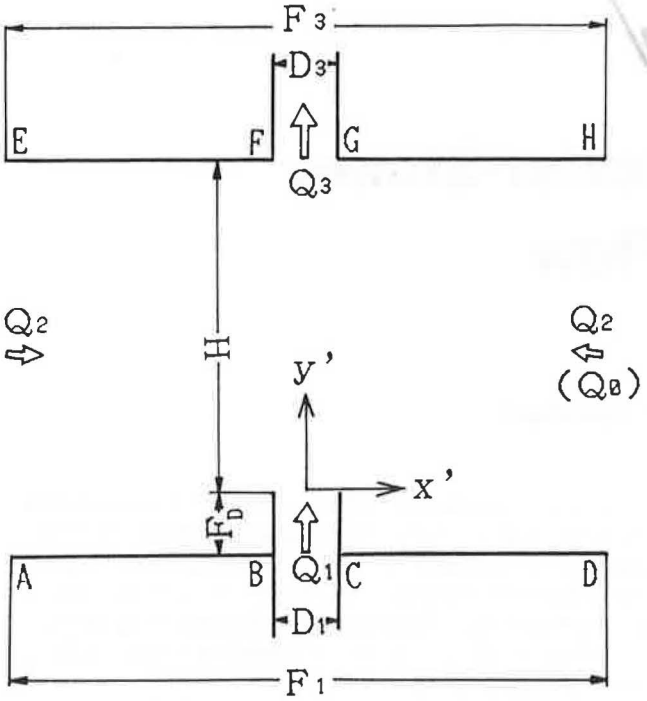

Figure 1 *Sketch of two-dimensional push-pull flow*

comparison of the two models shows that the results are different at the nozzle of the outlet or inlet where the turbulent velocity becomes violent. The computational accuracy of the k-ϵ model is better than that of the k-L model, while at a distance from the nozzle both results coincide well. Since the computational expense of the k-ϵ model is several times as much as that of the k-L model, the k-L model is used for turbulent flow in this paper. In addition to Equations 1, 2, and 3, the following equations are required for turbulent flows (Yoshikawa and Yamaguchi 1974):

$$\frac{\partial}{\partial x}\left(\omega\frac{\partial\psi}{\partial y}\right)-\frac{\partial}{\partial y}\left(\omega\frac{\partial\psi}{\partial x}\right)=\frac{\partial^2}{\partial x^2}\left(\nu_{eff}\omega\right)+\frac{\partial^2}{\partial y^2}\left(\nu_{eff}\omega\right)$$
$$-4\frac{\partial^2\psi}{\partial x\,\partial y}\frac{\partial^2\nu_{eff}}{\partial x\,\partial y}+2\frac{\partial^2\psi}{\partial y^2}\frac{\partial^2\nu_{eff}}{\partial x^2}+2\frac{\partial^2\psi}{\partial x^2}\frac{\partial^2\nu_{eff}}{\partial y^2} \tag{4}$$

$$\frac{\partial}{\partial x}\left(k\frac{\partial\psi}{\partial y}\right)-\frac{\partial}{\partial y}\left(k\frac{\partial\psi}{\partial x}\right)=\frac{\partial}{\partial x}\left(\nu_{k,eff}\frac{\partial k}{\partial y}\right)$$
$$+\nu_t\left\{4\left(\frac{\partial^2\psi}{\partial x\,\partial y}\right)^2+\left(\frac{\partial^2\psi}{\partial y^2}-\frac{\partial^2\psi}{\partial x^2}\right)^2\right\}-\sigma_0 k^{3/2}/L \tag{5}$$

$$\nu_{eff}=\frac{1}{Re}+\nu_t \tag{6}$$

$$\nu_{k,eff}=\frac{1}{Re}+\nu_t/\sigma_k \tag{7}$$

$$\nu_t=\sigma_\nu k^{1/2} L \tag{8}$$

For turbulent flows, the length scales, L, are designated as follows (Gosman et al. 1969):

If the distance from any solid face is Ln, then

$$L = Ln \text{ when } Ln \leqslant L\,max \tag{9}$$
$$L = L\,max \text{ when } Ln > L\,max \tag{10}$$
$$L\,max = \zeta L s \tag{11}$$
$$L s = (F_1 \times H)/2D_1^2 \tag{12}$$

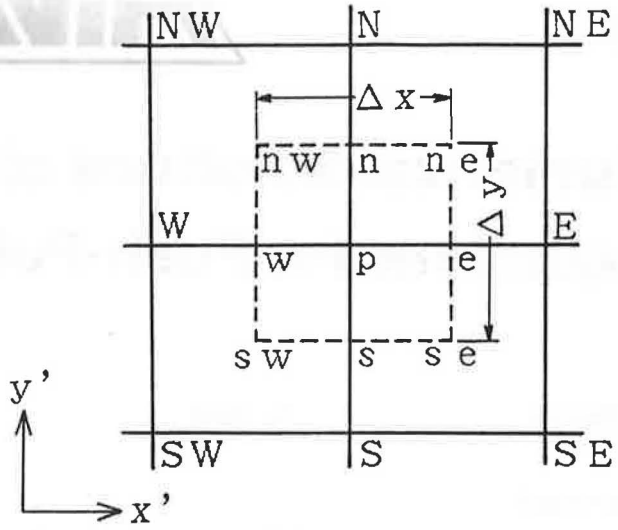

Figure 2 *Two-dimensional control volume*

The proportionality factor, ζ, is variable and can be determined by comparing the results of computation and experiment. However, in a certain limited calculation region, there is little effect of the change of ζ on the calculation results. Then, ζ is considered to be constant. It is of the order of magnitude 10^{-1}. The coefficients σ_D, etc., can be found in Table 1.

All these formulae are dimensionless. The width of the outlet, D_1, is used as the reference width, while the velocity at the outlet, V_1, is used as the reference velocity.

Finite Difference Expressions of Basic Equations

Figure 2 shows a two-dimensional grid. The grids are divided into uniform square meshes, i.e. $\Delta x = \Delta y$. The control volume around P is shown by dashed lines, and the points of e, w, n, and s are situated at the centers of EP, WP, NP and SP, respectively. Over the control volume in Figure 2 making the integrations of formulae (1), (2), (4), and (5), we can get the standard forms of the two-dimensional discretization equations (Patankar 1980):

$$a_P\phi_P = a_E\phi_E + a_W\phi_W + a_N\phi_N + a_S\phi_S + b \tag{13}$$

Then, the coefficients a_P, a_N, a_S, a_W, and a_E can be expressed in the form shown in Table 2. The expressions of coefficients b_E, A_E, ψ_{xy}, ν_{xy}, etc., can be found in Table 3.

Boundary Conditions

(a) For push opening: The values of all variables are assumed to be initial conditions.

(b) For pull opening: The normal gradients of all variables are assumed to be zero.

TABLE 1
Coefficient Values

σ_ν	σ_D	σ_k
0.22	0.416	1.53

TABLE 2
Definitions of Coefficients αE, αW, αN, αP & b

	Laminar Flows		Turbulent Flows		
ϕ_P	ψ_P	ω_P	ψ_P	ω_P	k_P
a_E	1	$b_E + \frac{1}{Re}$	1	$b_E + \nu_{eff.E}$	$b_E + A^k_E$
a_W	1	$b_W + \frac{1}{Re}$	1	$b_W + \nu_{eff.W}$	$b_W + A^k_W$
a_N	1	$b_N + \frac{1}{Re}$	1	$b_N + \nu_{eff.N}$	$b_N + A^k_N$
a_S	1	$b_S + \frac{1}{Re}$	1	$b_S + \nu_{eff.S}$	$b_S + A^k_S$
a_P	4	$\frac{4}{Re} + b_E + b_W + b_N + b_S$	4	$b_E + b_W + b_N + b_S + 4\nu_{eff.P}$	$b_E + b_W + b_N + b_S + A^k_E + A^k_W + A^k_N + A^k_S + \sigma_D k_P^{1/2} \Delta x \Delta y / L_P$
b	$\Delta x \Delta y \omega_P$		$\Delta x \Delta y \omega_P$	$\{-\psi_{xy}\nu_{eff.xy} + 1/2\,[\psi_{yy}\nu_{eff.xx} + \psi_{xx}\nu_{eff.yy}]\}\Delta x \Delta y$	$\nu_{t.P}\{4(\psi_{xy})^2 + (\psi_{yy}-\psi_{xx})^2\}$

(c) For solid wall:

1) Stream functions, ψ, are determined according to the ratio of flow rate.

2) Vorticities, ω, are given by the Woods method (Woods 1954), i.e.,

$$\omega_W = \frac{3(\psi_W - \psi_{W+1})}{\Delta n^2} - \frac{1}{2}\omega_{W+1} \qquad (14)$$

in which Δn is the distance from $(n + 1)$ to n perpendicular to the wall.

(d) Open boundary can be treated in either of the following ways:

1) Treated as general boundary: The boundary condition is similar to that of push opening.

2) Treated as free boundary: The boundary condition at the open face is first assumed to be an initial value. In the procedure of iteration to convergence, the value of a neighboring point evaluated by extrapolation is given to the boundary, leaving the boundary condition at free boundary unfixed for further improvements. In appearance, this is similar to the assumption of the boundary condition at the suction nozzle, but they are different in essence. For the pull opening, the boundary is at the lower bound of the calculated area, exerting no influence on the solution, while for the free boundary, the calculated points of the open face can be considered either at the lower bound or the upper bound, depending on the flow ratio. The difference of their influences on the solution is remarkable.

TABLE 3
Definition of Coefficients bE, ψxy, νeff.xx etc.

b_E	$\frac{1}{8}\{\psi_{SE} + \psi_S - \psi_{NE} - \psi_N + \lvert\psi_{SE} + \psi_S - \psi_{NE} - \psi_N\rvert\}$
b_W	$\frac{1}{8}\{\psi_{NW} + \psi_N - \psi_{SW} - \psi_S + \lvert\psi_{NW} + \psi_N - \psi_{SW} - \psi_S\rvert\}$
b_N	$\frac{1}{8}\{\psi_{NE} + \psi_E - \psi_{NW} - \psi_W + \lvert\psi_{NE} + \psi_E - \psi_{NW} - \psi_W\rvert\}$
b_S	$\frac{1}{8}\{\psi_{SW} + \psi_W - \psi_{SE} - \psi_E + \lvert\psi_{SW} + \psi_W - \psi_{SE} - \psi_E\rvert\}$
ψ_{xy}	$(\psi_{NE} - \psi_{NW} - \psi_{SE} + \psi_{SW}) / 4\Delta x \Delta y$
ψ_{xx}	$(\psi_E + \psi_W - 2\psi_P) / \Delta x^2$
ψ_{yy}	$(\psi_W + \psi_S - 2\psi_P) / \Delta y^2$
$\nu_{eff.xy}$	$(\nu_{eff.NE} - \nu_{eff.NW} - \nu_{eff.SE} + \nu_{eff.SW}) / 4\Delta x \Delta y$
$\nu_{eff.yy}$	$(\nu_{eff.W} + \nu_{eff.S} - 2\nu_{eff.P}) / \Delta y^2$
$\nu_{eff.xx}$	$(\nu_{eff.E} + \nu_{eff.W} - 2\nu_{eff.P}) / \Delta x^2$
A^k_E	$(\nu_{k.eff.E} + \nu_{k.eff.P}) / 2$
A^k_W	$(\nu_{k.eff.W} + \nu_{k.eff.P}) / 2$
A^k_N	$(\nu_{k.eff.N} + \nu_{k.eff.P}) / 2$
A^k_S	$(\nu_{k.eff.S} + \nu_{k.eff.P}) / 2$

Convergence Criterion

The variables ψ, ω, and k on the free boundary vary with every iteration of calculation and are hard to converge. Besides, the variables ψ, ω, and k on the general boundary do not change with iteration of calculation and are easy to converge.

Then, the convergence criterion of iteration is as follows without distinction of free or general boundary:

a) The convergence criterion is previously fixed, $\Delta = 10^{-4}$

b) In the SOR (successive over-relaxation) method, maximum iteration is decided as follows, $N_{max} = 1000$.

When the ratio of a maximum of absolute correction values on every point to a maximum of absolute variable values is less than Δ in any case of ψ, ω, and k, respectively, the numerical calculation is considered to converge.

EXPERIMENTAL PROCEDURES

For measuring the velocity and flow direction of push-pull flows, the smoke wire method and hot-wire anemometer are used.

Smoke Wire Method

A machine oil with paraffin oil added is painted on a nicrome wire, which is stretched perpendicularly to flow direction. When the electric current flows on the wire

momentarily, vapor of paraffin oil touches the airflow at normal temperature and condenses back to mist by cooling. The airflow through the wire can be visualized by the mist.

After the electric current flows, the airflows are illuminated in a proper time lag with a stroboscope and are photographed. The velocity distributions near the wire are visualized as the time line of the mist.

Hot-Wire Anemometer Method

The probe of the hot-wire anemometer is inserted into the side opening. The velocity of push-pull flows can be measured by means of the probe traversing to the x or y direction.

COMPARISON OF RESULTS

Evaluation of the Minimum Flow Ratio

The ratio of flow rate is defined as:

$$K = K_{min} = Q_3/Q_1 = (Q_1 + Q_2)/Q_1 = 1 + (Q_2/Q_1) \qquad (15)$$

It can be determined in the following way:

When the push-pull flow has not been set out, the surrounding air can be considered steady. Then, Q_2 in Equation 15 is the surrounding air entrained by the push-pull flow. When $Q_3/Q_1 = 1$, then $Q_2 = 0$, meaning that the flow entrained from the opening AE and DH will return back to the surroundings from the same openings. Accordingly, the minimum flow ratio, K_{min}, can be determined by checking the directions of the flow at AE and DH. For quicker computation time, the push-pull flow can be assumed to be symmetric about the center line. Then, only half of the computated area is to be taken into consideration and, in this case, the flow function and the vorticity at the symmetric axis will be equal to zero.

Figure 3 shows an example for determining the minimum flow ratio, K_{min}, of laminar flow. Figures 3a and 3b indicate the case when $K > K_{min}$, the flow, Q_2, is drawn into the opening AE totally or partially returns to the surroundings from the same opening. In another case (Figure 3c), when $K < K_{min}$, the flow, Q_2, is drawn in from the opening AE and proceeds forward without turning around. In the meantime, the result from the computational analysis is $K_{min} = 1.21$.

Figure 4 shows the visualized time lines obtained by using the smoke wire method for the verification of the calculated results of Figure 3. Although the results of visualized experiments are influenced by the buoyancy and cannot sufficiently embody the direction of individual streams, they do reflect the flow as a whole and can be used to ascertain the location and amount of the adverse current. From the comparison between numerical calculations and experiments, it can be concluded that the free boundary method and the method for determining minimum flow ratio are feasible.

Since the practical flows are turbulent and the gases isolated by push-pull flows always possess a certain velocity, the formula that is more useful than Equation 15 can be written as:

$$K = K_{min} = Q_3/Q_1 = (Q_0 + Q_1 + Q_2)/Q_1$$
$$= (Q_0/Q_1) + (Q_2/Q_1) + 1 \qquad (16)$$

where Q_0 is the quantity of gas to be isolated. Isolated gases are side flows and are assumed to be uniformly produced.

The examples of minimum flow ratio for turbulent flow shown in Figure 5 include cases when $K < K_{min}$ (Figures 5a and 5b) and when $K > K_{min}$ (Figure 5c). By reference to

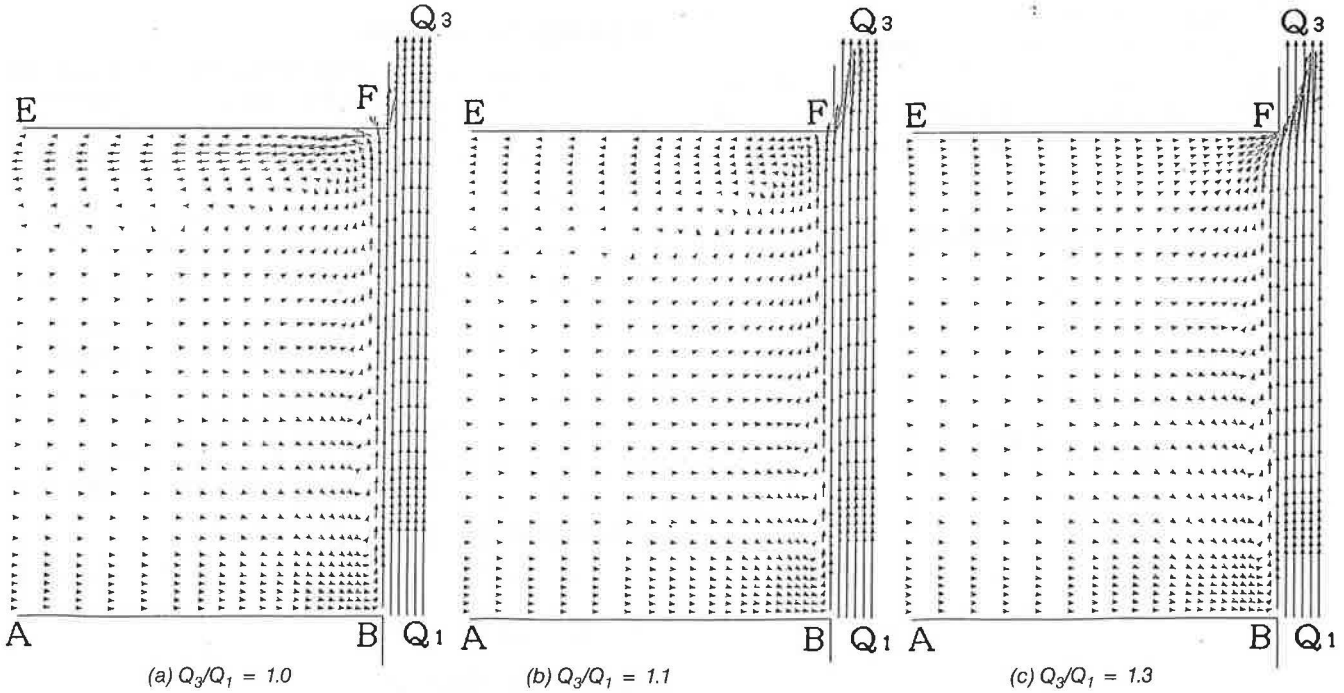

(a) $Q_3/Q_1 = 1.0$

(b) $Q_3/Q_1 = 1.1$ when $K = Q_3/Q_1 < K_{min}$

(c) $Q_3/Q_1 = 1.3$ when $K = Q3/Q1 \times K_{min}$

Figure 3 *Velocity vector diagrams of laminar push-pull flow ($F1/D1 = 10.0$, $H/D_1 = 6.0$)*

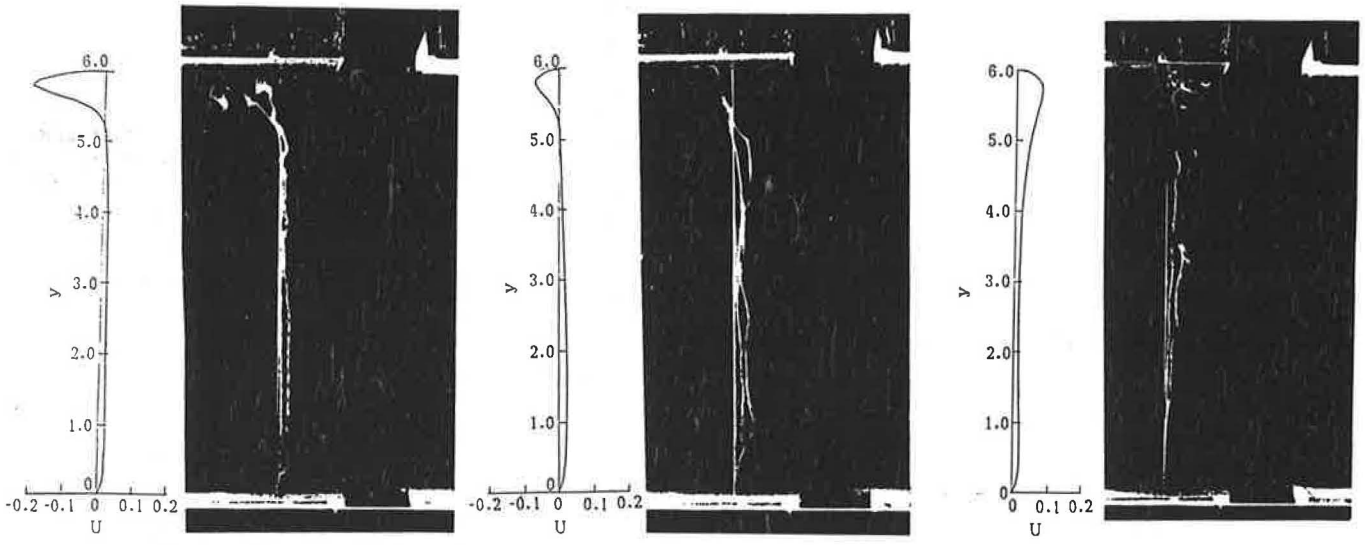

(a) Q_3/Q_1 = 1.0 (b) Q_3/Q_1 = 1.1 (c) Q_3/Q_1 = 1.3

Figure 4 *Comparisons between calculations and experiments for laminar flow*

(F_1/D_1 =10.0, H/D_1 = 6.0, x/D_1 = 1.4)

Figures 5b and 5c, it can be seen that the minimum flow ratio, K_{min}, is in the range of 1.8 to 2.0 in the case of Q_0/Q_1 = 0.5. For any isolated gas quantity, Q_0, the minimum flow ratio can be obtained by this method.

For turbulent flows, it is not enough to determine the flow ratio according to whether there is leakage. The correct way is to determine the minimum flow ratio according to the amount of adverse current or the circulating flow under the upper flange (shown in Figure 5b).

Effect of a Flange Equipped on an Opening of Push Flow

The effect of the flange by the outlet on the fluidity of flow can hardly be explained in a few words. Apparently, since the resistance of the flange to surrounding air carried along with the outlet flow will consume some kinetic energy, the installation of flanges is not preferable in engineering practice. However, the wall around the outlet of an air-conditioned room and a plate similar to the flange will inevitably exist for the presence of connecting structures.

Then, the numerical analysis method can be used to find the rational extension length of the outlet to minimize the effect of the flange.

Now, a laminar flow problem will be mentioned. For the case when Q_3/Q_1 = 2, H/D_1 = 2.5, and Re = 3000 are fixed, while F_D increases by 0.125 D_1, plotting the distribution lines of velocities at four sections in the cases of y = 0.1, 0.75, 1.5, and 2.2 between the outlet and inlet, one can analyze the distribution of velocities at the section for each y to ascertain the effect of the flange on the fluidity

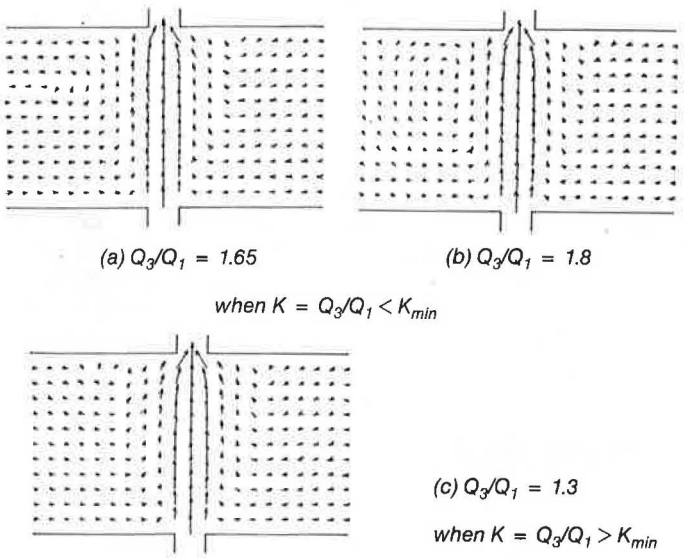

(a) Q_3/Q_1 = 1.65 (b) Q_3/Q_1 = 1.8

when $K = Q_3/Q_1 < K_{min}$

(c) Q_3/Q_1 = 1.3

when $K = Q_3/Q_1 > K_{min}$

Figure 5 *Flow vector diagram of turbulent push-pull flow*

(F_1/D_1 = 10.0, H/D_1 = 6.0, $Q0/Q_1$ = 0.5)

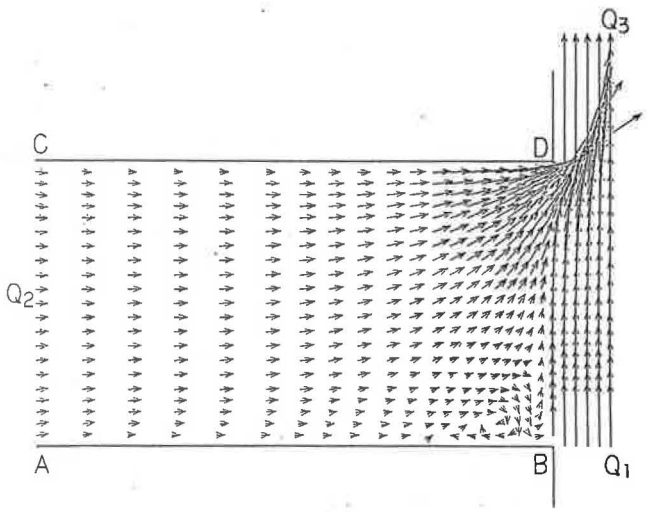

Figure 6 *Velocity vector diagram (FD/D_1 = 0, Q_3/Q_1 = 2, H/D_1 = 2.5)*

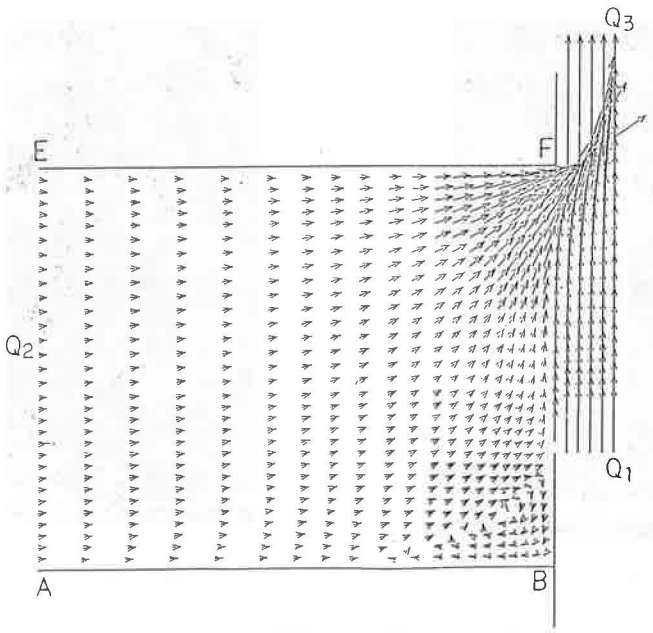

Figure 7 *Velocity vector diagram (FD/D_1 = 1.0, Q_3/Q_1 = 2, H/D_1 = 2.5)*

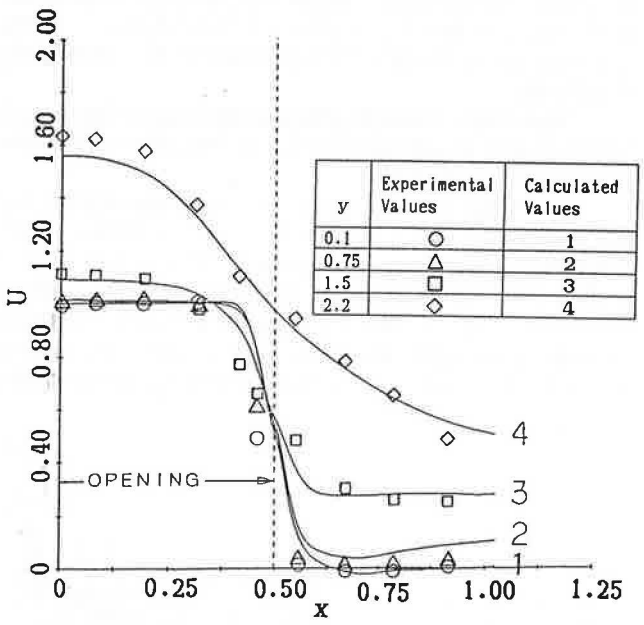

Figure 8 *Comparison between calculations and experiments when FD/D_1 = 0*

of outlet flow. Calculation results indicate that when $F_D = D_1$, the effects of flange on the fluidity of outlet flow become steady.

Figures 6 and 7 show the velocity vector diagrams for F_D = 0 and $F_D = D_1$, respectively. Figures 8 and 9 indicate the calculated and experimental values, and are the velocity distributions at relevant sections taken from Figures 6 and 7. Since y = 0 denotes the region of the outlet, y = 2.5, one of the inlets, section 4, is near the inlet

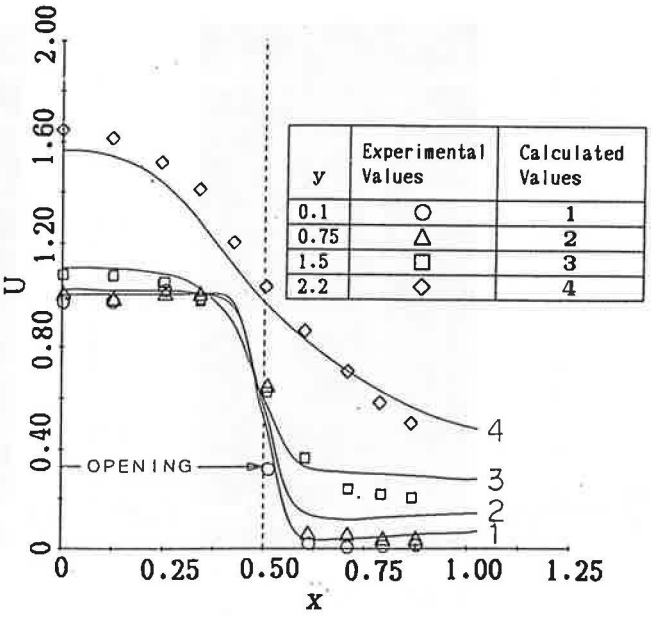

Figure 9 *Comparison between calculations and experiments when FD/D_1 = 1*

region. Therefore, U values at section 4 are affected by the suction stream and become large, as is shown in Figures 8 and 9.

The velocity distribution lines for y = 0.1 and y = 0.75 in Figure 8 are distinctly lower than those in Figure 9. The discrepancy is due to the effect of flange. Thus, a conclusion can be drawn that if the outlet is extended, the velocity of the flow by the outlet can be increased. The velocity distributions of the sections in Figures 8 and 9 have been verified by experiments.

CONCLUSIONS

The concept of free boundary of the push-pull flow and the method for determining the minimum flow ratio were first discussed in this paper. The comparison between the calculations and the experiments proved the validity of the free boundary method. For the criterion of the minimum flow ratio, the authors prefer the location of adverse current rather than the leakage at the opening AE. This idea is subject to more experimental proofs for more complicated cases.

In the case when there is a flange by the outlet, the disadvantageous effects of the flange can be eliminated as long as the outlet is extended a certain distance from the flange. The extended length is a function of the flow ratio and the geometric form of the push-pull installation. The method for solving this kind of problem has been revealed in this paper.

NOMENCLATURE

D_1 = width of outlet (m)
D_3 = width of inlet (m)
F_1 = full length of flange at outlet (m)
F_3 = full length of flange at inlet (m)
F_D = extension length of outlet (m)
H = distance between outlet and inlet (m)

Q_0 = quantity of side flow (m^3/s)
Q_1 = quantity of outlet (m^3/s)
Q_2 = quantity of flow surroundings (m^3/s)
Q_3 = quantity of inlet (m^3/s)
K = ratio of flow rate (= Q_3/Q_1)
Re = Reynolds number
U = dimensionless velocity (when $u \geq 0$, $U = \sqrt{u^2 + v^2}$)
(when $u < 0$, $U = -\sqrt{u^2 + v^2}$)
u = component of U in x-direction (= u'/V_1)
v = component of U in y-direction (= v'/V_1)
V_1 = outlet velocity (m/s)
x = dimensionless abscissa (= x'/D_1)
y = dimensionless ordinate (= y'/D_1)
ν = coefficient of kinetic viscosity (m^2/s)
ψ = dimensionless stream function (= ψ'/V_1D_1)
ω = dimensionless vorticity (= $'D_1/V_1$)
k = kinetic turbulent energy
L = length of energy-containing eddies
σ_D, σ_k, σ_ν = coefficients
$'$ = dimensionality

REFERENCES

Damin Z., and Xinghua, W. 1986. "Comparison of k-L model with k-ϵ model in the numerical solution of turbulent gas-flow." *Journal of Hunan University*, Vol. 13, No. 4, pp. 111-119.

Gosman, A.D.; Pun, W.N.; Runchal, A.K.; Spalding, D.B.; and Wolfshtein, M. 1969. *Heat and mass transfer in recirculating flows*. London: Academic Press.

Hayashi, T.; Howell, R.H.; Shibata, M.; and Tsuji, K. 1985. *Industrial ventilation and air conditioning*. Boca Raton, FL: CRC Press.

Patankar, S.V. 1980. *Numerical heat transfer and fluid flow*. New York: McGraw-Hill.

Woods, L.C. 1954. "A note on the numerical solution of four order differential equations." *Aeronautical Quarterly*, Vol. 5, Part 3, p. 176.

Yoshikawa, A., and Yamaguchi, K. 1974. "Numerical solution of room air distribution, part 2." *Journal of Society of Heating, Air Conditioning and Sanitary Engineers of Japan*, Vol. 48, No. 1, pp. 5-17.